Proceedings World Geothermal Congress 2010
Bali, Indonesia, 25-29 April 2010

# Passive Seismic Monitoring: Mapping Enhanced Fracture Permeability

Elmar Rothert and Stefan Baisch

Q-con GmbH, Markstr. 39, D-76887 Bad Bergzabern, Germany

rothert@q-con.de, baisch@q-con.de

**Keywords:** passive seismic monitoring, stimulation, seismo-hydraulic analysis

## ABSTRACT

The economical performance of a geothermal reservoir strongly depends on how accurate the *in situ* hydraulic conductivity can be determined. Averaged reservoir conductivity and near-well hydraulic properties can be determined by well test analyses. However, direct monitoring of hydraulic parameters further away from wells remains a challenging task.

We present a new technique for spatially mapping regions of enhanced hydraulic conductivity in EGS (Enhanced Geothermal Systems) reservoirs. Our approach is based on the concept of self-propping of fractures that experienced shear-deformation during hydraulic stimulation. These deformation processes radiate seismic signals ("microearthquakes") which carry information on the location and the amount of shear displacement that occurred in the reservoir. By mapping the (cumulative) shear deformation of stimulation induced seismicity, a detailed 3-D image of the stimulated reservoir is obtained.

We apply the approach of cumulative shear slip mapping (CSSM) to a field data example in the Cooper Basin EGS reservoir (Australia). During stimulation activities, about 45,300 microseismic events were induced from which approximately 32,200 could be located. Seismic activity aligns along a single, subhorizontal fault. Cumulative slip determined by mapping the slip contribution of individual events onto the fracture zone indicates that most fracture patches in the reservoir slipped repeatedly, accumulating up to several centimetres of shear displacement. Based on CSSM we have determined an optimum location for a new production well in the Cooper Basin reservoir. This well was successfully completed in 2008 and exhibits excellent connectivity to the reservoir.

## 1. INTRODUCTION

Aside from volcanic regions, most places in the world do not exhibit natural geological structures where temperature and rock-permeability meet the conditions required for a geothermal power production. The EGS (Enhanced Geothermal Systems) concept implies the creation of an artificial subsurface heat exchanger by enhancing the rock permeability in a spatially confined region. Such reservoir stimulation is achieved by injecting large volumes of fluid into the host rock under high pressures.

Averaged permeability enhancement achieved by hydraulic stimulations can be determined by well test analysis. Figure 1 shows data collected during a hydraulic stimulation experiment at the geothermal reservoir Bad Urach, Germany. Well test analysis has been used to predict the response of the reservoir to the hydraulic injection. The predicted response of the system started deviating from observed data as soon as induced seismicity started. At this point in time, hydraulic conductivity was (locally) increased resulting in smaller well-head pressures. These observations demonstrate a direct relationship between induced seismicity and hydraulic conductivity enhancement. The well test analysis, however, provides only (spatially) averaged reservoir properties. A major challenge in EGS technology is an optimum positioning of the injection and production wells with respect to the stimulated zones. This is critically dependent on the spatial image of *in situ* hydraulic conductivity. In the current paper we present a new technology for determining 3-D images of enhanced reservoir conductivity.

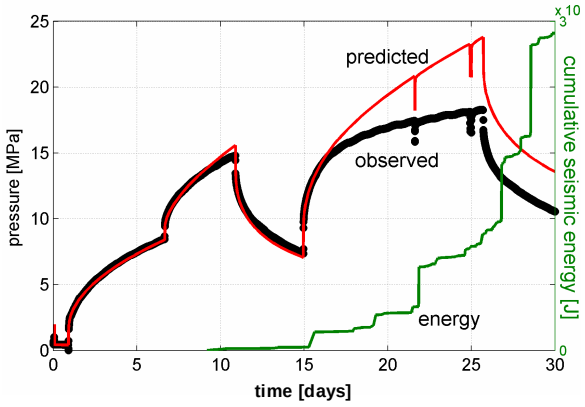


**Figure 1: Predicted (red) and observed (black) hydraulic response during an injection test at the geothermal reservoir Bad Urach. Cumulative seismic energy is annotated in green. Deviations from the predicted hydraulic response (based on pre-stimulation well-test analysis) closely follow the onset of induced seismicity indicating local changes of hydraulic parameters (permeability enhancement).**

## 2. HYDRAULIC STIMULATION AND SEISMIC ACTIVITY

### 2.1 Self Propping

Depending on rock properties and stress conditions, different types of mechanical processes may cause an increase of the permeability. Above the jacking pressure (i.e. the least principal stress), hydrofracturing or hydraulic opening of pre-existent fractures can lead to a substantial permeability increase. However, to keep artificially jacked fractures open after the release of the stimulation pressure, the addition of proppants to the injected fluid is frequently required.

In the EGS context the addition of proppants is usually not practicable because of their limited penetration depth and their relatively high costs. Instead, the EGS concept relies mainly on the effect of natural or "selfpropping" (Jung, 1987), which occurs below the jacking-pressure. The underlying principle is based on shear displacement along

fracture surfaces. After the pressure is released, the fractures do not collapse but retain a certain rest aperture due to the irregular, rough nature of the displaced fracture surfaces ("retained permeability"). This is illustrated in Figure 2 showing a natural fracture in a granite core. With only a few millimetres of shear displacement, fracture aperture (and thus hydraulic conductivity) was substantially increased.

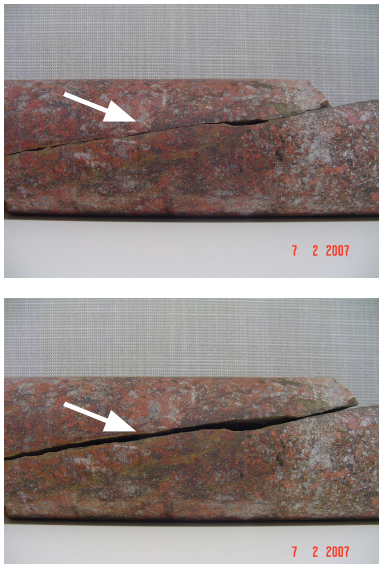


**Figure 2: Granite core with a natural fracture (arrow). With only a few millimetres of shear displacement, fracture aperture has substantially increased (bottom).**

Laboratory measurements confirm this process. In Figure 3 permeability enhancement of a fracture is plotted versus shear displacement at different confining pressures (data after Chen et al., 2000). A clear trend of increasing permeability with increasing shear displacement can be observed.

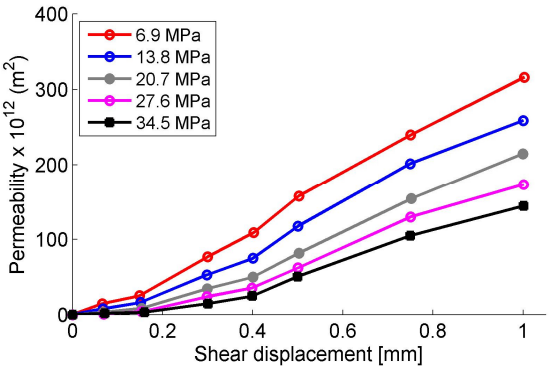


**Figure 3: Results of laboratory experiments after Chen et al., 2000. Permeability enhancement of a fracture is plotted versus the shear displacement at different confining pressures. Permeability increases with shear displacement.**

Since the shearing process is accompanied by the emission of seismic waves (microearthquakes), the location of induced seismicity indicates where the reservoir conductivity has been enhanced.

### 2.2 Direct Monitoring: Seismicity Based Reservoir Characterization (SBRC)

In a number of previous studies, the spatial distribution of hypocenters of induced seismicity is directly associated with fracture systems and their hydraulic characteristics (e.g., Phillips et al., 1997; Shapiro et al., 1997; Moriya et al., 2002). Several approaches have been suggested to analyze systematic structures within hypocenter distributions (e.g., Fehler et al., 1987; Jones and Stewart, 1997; Nicholson et al., 2000), which are commonly interpreted as hydraulically relevant features. By this, all hypocenters are treated as equivalent points neglecting their individual physical properties.

In addition characterizing hydraulic fracture growth, microseismicity has been used for estimating hydraulic properties over large scales. Shapiro et al. (1997, 2002) introduced an approach (Seismicity Based Reservoir Characterization, SBRC) which assumes that microseismicity is triggered by a diffusive process of pore pressure relaxation. The proposed approach yields estimates of hydraulic parameters such as hydraulic diffusivity and permeability on a large spatial scale (Figure 4 and Figure 5). This approach was successfully applied to various data sets from hydraulic injection experiments as well as to synthetic data sets (Rothert and Shapiro 2003; Rothert, 2004).

Although the SBRC approach provides important estimates of the hydraulic diffusivity, it does not consider the individual (physical) properties of induced microearthquakes. From the previous section it is clear that the amount of shear deformation is the key parameter describing permeability enhancement. In principle, this information is contained in seismogram recordings as will be discussed in the following section.

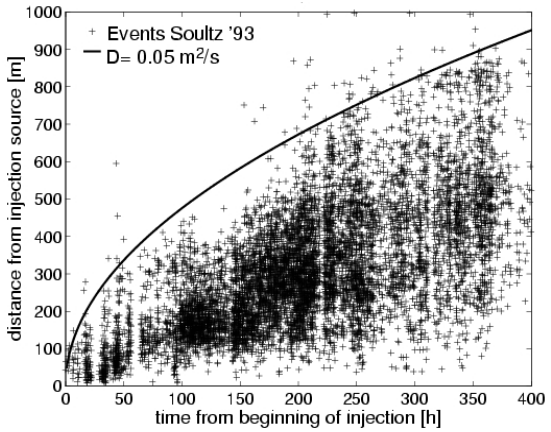


**Figure 4: Scalar estimate of hydraulic diffusivity from induced microseismicity during a stimulations experiment in the year 1993 at Soultz-sous-Forêts, France. Diffusivity is estimated by the outer envelope in a plot of event occurrence time versus scalar distance relative to the injection source. Taken from Shapiro et al. (2002).**

### 2.3 Direct Monitoring: Cumulative Shear Slip Mapping

Until here we have shown that induced shear slip can be used for estimating hydraulic conductivity enhancement. In order to determine the shear slip of an individual seismic event, the relationship of seismic moment and the product of area and slip can be used (e.g., Aki and Richards, 2002)

$$M_0 = G \cdot A \cdot d \qquad (1)$$

where $G$ corresponds to the shearing modulus, $A$ to the area and $d$ to the average slip. Seismic moment can be directly derived from seismogram recordings with reasonable accuracy. Practically, the trade-off between source area and shear slip in equation (1) can not be resolved without *a priori* assumptions on the event geometry. In a first order approach we may assume a circular slip area with a homogeneous slip distribution yielding an image as shown in Figure 6 (bottom). Clearly, mapping the slip on circular patches is an improvement compared to the classical point cloud display (Figure 6, top); however, the resulting image might be strongly biased by the a priori assumption of circular fracture planes.

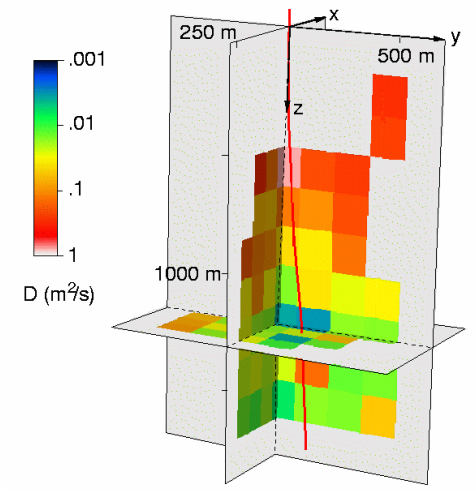


**Figure 5: Spatial reconstruction of hydraulic diffusivity using the SBRC approach for the Soultz 1993 data set (Shapiro et al., 2002).**

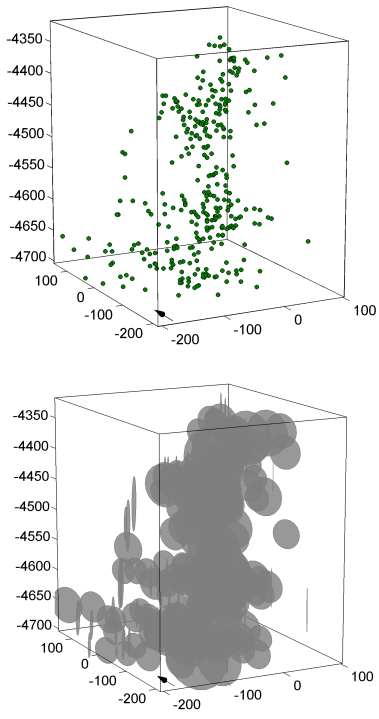


**Figure 6: Hypocenters of induced events visualized as a point cloud (top) and scaled to shearing area (bottom). Shearing on circular patches has been assumed a priori.**

In the special case of multiple, neighbouring earthquakes with overlapping source area, the uncertainty in either the slip or the slip area tends to average out when cumulative slip is considered (Figure 7). For large, overlapping data sets, the cumulative shear slip maps thus provide a stable estimator of the actual shear slip, independent of the assumed source geometry.

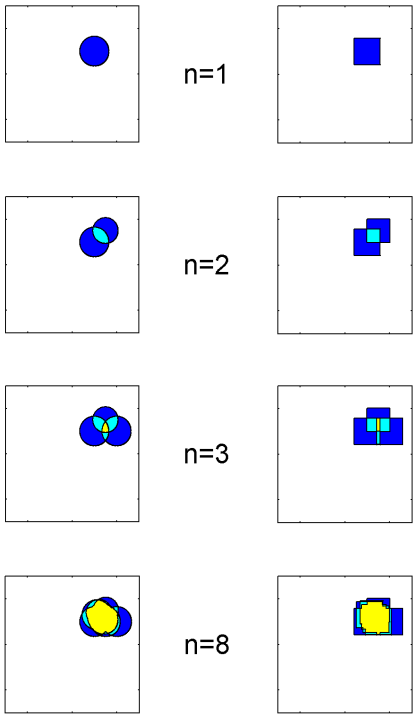


**Figure 7: Cumulative slip display for different source geometries (left: circular shearing, right: shearing on rectangles). With increasing number of shear events, the uncertainty in source geometry averages out.**

## 3. CASE STUDY: CUMULATIVE SHEAR SLIP MAPPING IN THE COOPER BASIN RESERVOIR

The Cooper Basin geothermal field is located in the northeast of South Australia near the Queensland border (see Figure 8). Geothermal exploration started in the year of 2002, and to date three deep wells have been drilled into the granite to a depth level of 4200–4400 m.


**Figure 8: Location of the Cooper Basin geothermal site in South Australia.**

To enhance the hydraulic permeability between the injection well, Habanero#1, and the production well, Habanero#2, the injection well was hydraulically stimulated in 2003 and in 2005, respectively. Thereby about 45,000 induced microearthquakes were detected. Baisch et al. (2006, 2009) demonstrate that the induced seismicity aligns along a single, subhorizontal fracture zone (Figure 9). Logging data acquired before the stimulation indicate that the fracture zone is of natural (tectonic) origin and already existed before reservoir activities started in the Cooper Basin.

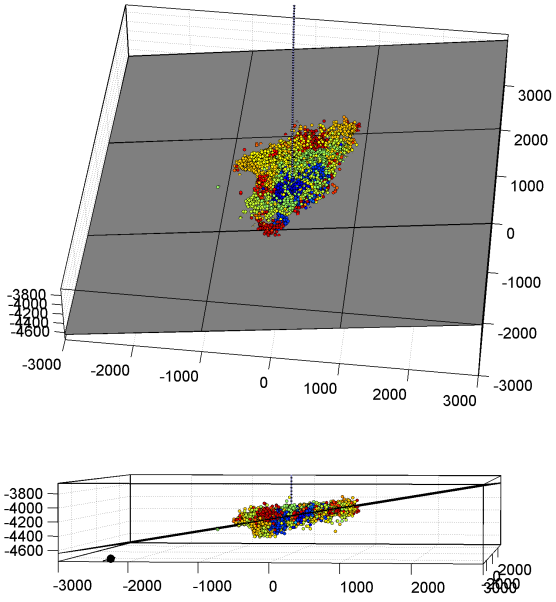


**Figure 9: Cloud of induced seismic in the Cooper Basin, Australia in perspective (top) and side view (bottom). Color corresponds to the event occurrence time. The gray area denotes the best fitting plane determined from the hypocenter distribution.**

For this scenario, one could expect very similar source mechanisms for the induced seismicity. Indeed, the analysis of P-wave polarity data indicates extremely similar fault mechanisms for the entire data set, which is consistent with only two different fracture orientations (see Figure 10). Compound fault-plane solutions for the two associated event types indicate that both event types are driven by the regional stress field with maximum stress oriented west-northwest / east-southeast (Figure 11). Fault planes of both event types are dipping at a relatively low angle, which is typically observed for large-scale thrust faults. The intersection angle of 21° between the type I and type II fault planes might indicate that the planes have formed as conjugated fractures with the dominating type I events representing a connected, large-scale feature being locally intersected by type II fractures.

For the current data set, all seismicity occurs on a single layer structure and predominantly exhibits the same slip direction. Therefore, the cumulative shear slip associated with multiple events can be estimated by simply adding the individual slip contribution of events with overlapping source area. To quantify the cumulative slip induced by stimulation activities in the Habanero#1 well, we used empirical relations to estimate source parameters for all events recorded between 6 November 2003 and 13 November 2005.

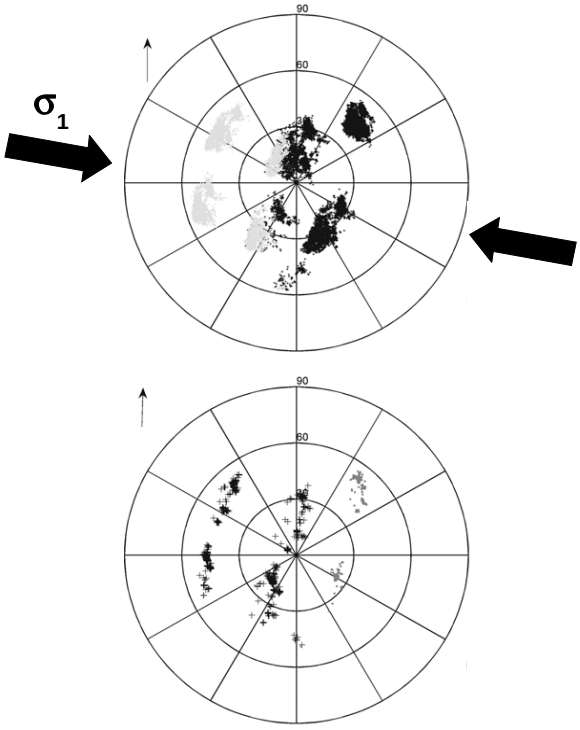


**Figure 10: Stereographic projection of azimuth and incidence of type I events (top) and type II events (bottom). Dark colour corresponds to positive and grey colour to negative polarity, respectively.**

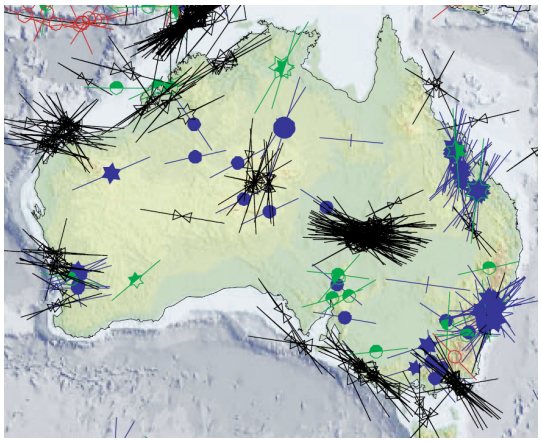

**Figure 11: Regional stress field of Australia. Taken from the world stress map project. Main stress direction $\sigma_1$ is nearly east-west.**

We applied the circular crack model of Brune (1970) to estimate the source area and slip from the seismic moment.

Figure 12 shows the resulting distribution of the cumulative slip. The injection well is surrounded by a high slip region where cumulative slip locally exceeds 9 cm. Slip contributions of individual events are in the range of 0.03–21 mm, indicating that most regions of the reservoir slipped repeatedly for a considerable number of times. The high slip region in the central part of the reservoir exhibits some topography, but cumulative slip values larger than, say, 3 cm are consistently observed along a connected structure with a lateral extension of about 2500 m.

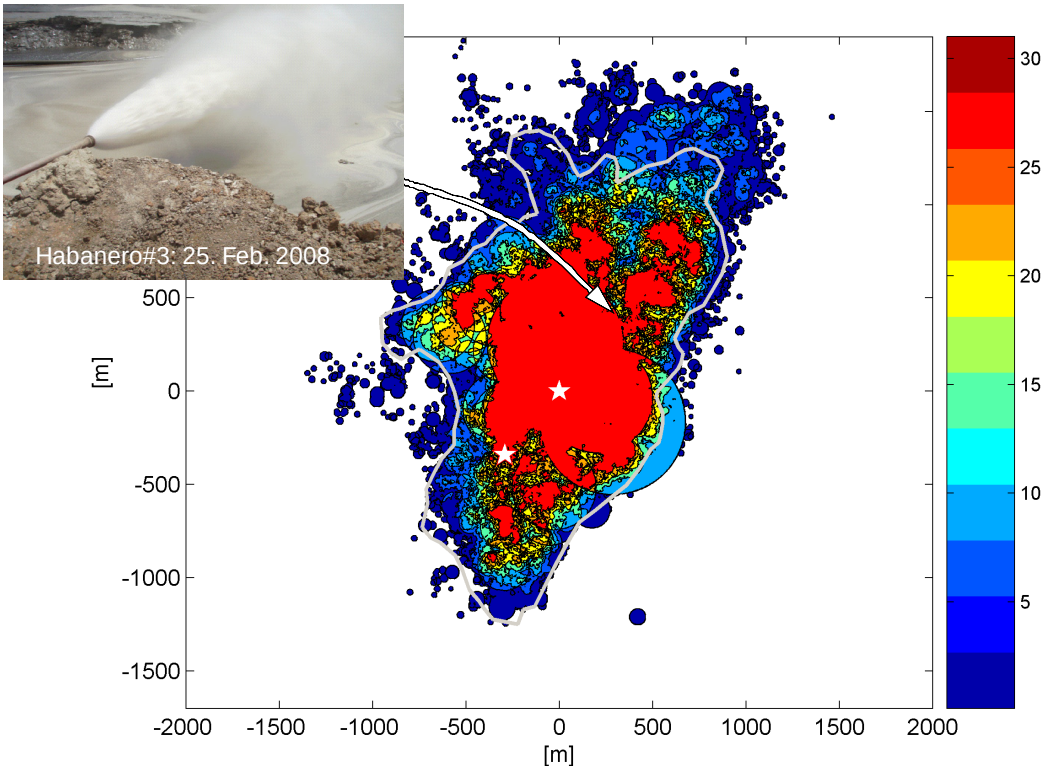


**Figure 12: Cumulative shear slip map of the Cooper Basin reservoir in map view. Shear slip is displayed in millimetres according to the colormap and is saturated at 30 mm. White stars denote the location of the wells Habanero#1 and Habanero#2. Based on this slip map, an optimum target for the Habanero#3 production well (white arrow) has been determined. Inset shows production from Habanero#3 immediately after drilling into the fracture zone.**

This slip map has been used for determining an optimum wellbore target for the new production well, Habanero#3. It should be noted that an exact relationship between shear slip and permeability is not known and cannot simply be extrapolated from the laboratory scale (**Figure 3**). Therefore, we considered the Habanero#2 location where hydraulic conductivity and cumulative shear slip are accessible ("calibration point"). The shear slip map in

Figure 12 has been saturated at the amount of slip observed at the Habanero#2 location. Taking into account constraints from thermo-hydraulic modelling (Q-con report to Geodynamics Limited, confidential), an optimum wellbore target has been determined near the outer rim of the highly stimulated zone (

Figure 12). Habanero#3 has successfully been completed in February 2008 and exhibits excellent connectivity to the stimulated reservoir.

## 4. CONCLUSIONS

Based on the concept of self-propping of fractures during hydraulic stimulation, we developed a new technique for spatially mapping regions of enhanced hydraulic conductivity in reservoirs (Cumulative Shear Slip Mapping, CSSM). The approach was applied to data from the Cooper Basin (Australia) geothermal reservoir. Cumulative shear displacement in the reservoir is as large as several centimetres near the injection well.

Based on CSSM we have determined an optimum location for a new production well in the Cooper Basin reservoir. This well was successfully completed in 2008 and exhibits excellent connectivity to the reservoir.

## REFERENCES

Aki, K., and P. G. Richards (2002). Quantitative Seismology, Second Ed., *Univ. Science Books*, Sausalito, California.

Baisch, S., Vörös, R., Weidler, R. and Wyborn, D., 2009, Investigation of Fault Mechanisms during Geothermal Reservoir Stimulation Experiments in the Cooper Basin (Australia). Bull. *Seism. Soc. Amer.*, 99 (1), 148-158.

Baisch, S., R. Weidler, R. Vörös, D. Wyborn, and L. DeGraaf (2006). Induced seismicity during the stimulation of a geothermal HFR reservoir in the Cooper Basin (Australia), *Bull. Seismol. Soc. Am.* 96, 2242–2256.

Brune, J. (1970). Tectonic stress and the spectra of seismic shear waves from earthquakes, *J. Geophys. Res.* 75, 4997–5009.

Chen, Z., S. P. Narayan, Z. Yang, and S. S. Rahman (2000). An experimental investigation of hydraulic behaviour of fractures and joints in granitic rock, *Int. J. Rock Mech. Min. Sci.* 37, 1061–1071.

Fehler, M., L. House, and H. Kaieda (1987). Determining planes along which earthquakes occur: method and application to earthquakes accompanying hydraulic fracturing, *J. Geophys. Res.* 92, no. B9, 9407–9414.

Jones, R. H., and R. C. Stewart (1997). A method for determining significant structures in a cloud of earthquakes, *J. Geophys. Res.* 102, no. B4, 8245–8254.

Jung, 1987. "Propagation and Hydraulic Testing of a Large Unpropped Hydraulic Fracture in Granite". *Geologische Jahrbücher*, E 39, 37-65.

Moriya, H., N. Katsuhisa, H. Niitsuma, and R. Baria (2002). Detailed fracture system of the Soultz-sous-Forêts HDR field evaluated using microseismic multiplet analysis, *Pure Appl. Geophys.* 159, 517–541.

Nicholson, T., M. Sambridge, and O. Gudmundsson (2000). On entropy and clustering in earthquake hypocentre distributions, *Geophys. J. Int.* 142, 37–51.

Phillips,W. S., L. S. House, and M. C. Fehler (1997). Detailed joint structure in a geothermal reservoir from studies of induced microearthquake clusters, *J. Geophys. Res.* 102, no. B6, 11,745–11,763.

Rothert, E., and S. Shapiro (2003), Microseismic monitoring of borehole fluid injections: Data modeling and inversion for hydraulic properties of rocks, *Geophysics*, 68(2), 685– 689.

Rothert, E. (2004), Fluid induced microseismicity: Data modeling and inversion for hydraulic properties of rocks, *Ph.D. thesis*, Freie Univ., Berlin.

Shapiro, S., E. Huenges, and G. Borm (1997). Estimating the crust permeability from fluid-injection-induced seismic emission at the KTB site, *Geophys. J. Int.* 131, F15–F18.

Shapiro, S. A., E. Rothert, V. Rath, and J. Rindschwentner (2002), Characterization of fluid transport properties of reservoirs using induced microseismicity, *Geophysics*, 67, 212–220.